iScience

CellPress
OPEN ACCESS

Article

Salivary exosomes exacerbate colitis by bridging the oral cavity and intestine

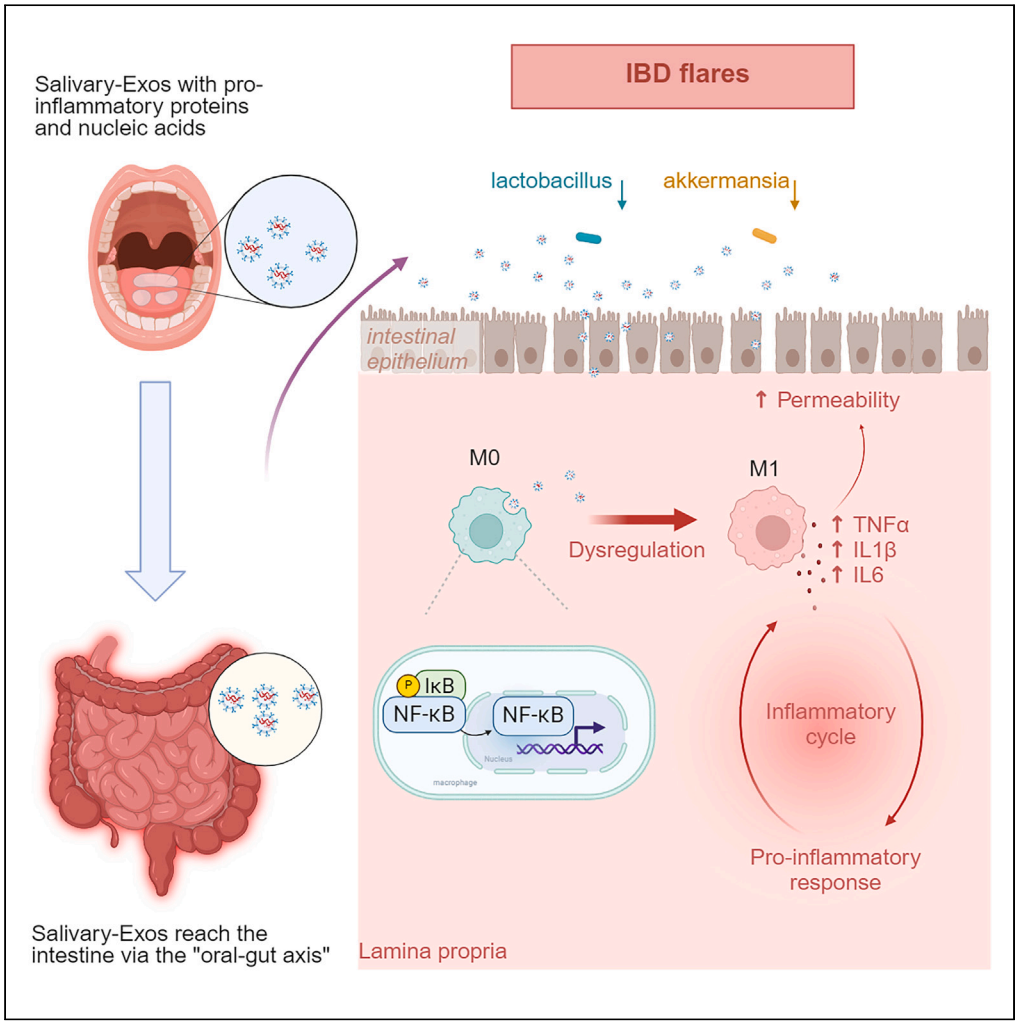

Congyi Yang, Jingyi Chen, Yuzheng Zhao, ..., Feng Chen, Yang Chen, Ning Chen

chenfeng2011@hsc.pku.edu.cn (F.C.)
chenyang1816185048@bjmu.edu.cn (Y.C.)
chenning79@bjmu.edu.cn (N.C.)

Highlights

Salivary exosomes play a significant role in oral-gut axis

Salivary exosomes from active IBD patients (active IBD-Sexos) aggravate the colitis

Active IBD-Sexos can disrupt the intestinal epithelial barrier, and modulate gut immunity

35 differentially expressed microRNAs in active IBD-Sexos

Yang et al., iScience 27, 111061
November 15, 2024
https://doi.org/10.1016/j.isci.2024.111061

iScience

CellPress
OPEN ACCESS

Article

Salivary exosomes exacerbate colitis by bridging the oral cavity and intestine

Congyi Yang,[1] Jingyi Chen,[1] Yuzheng Zhao,[1] Jushan Wu,[1] Yalan Xu,[1] Jun Xu,[1] Feng Chen,[2,*] Yang Chen,[3,*] and Ning Chen[1,4,5,*]

SUMMARY

Inflammatory bowel disease (IBD) presents a range of extraintestinal manifestations, notably including oral cavity involvement. The mechanisms underlying oral-gut crosstalk in IBD are not fully understood. Exosomes, found in various body fluids such as saliva, play an unclear role in IBD that requires further exploration. In the dextran sulfate sodium (DSS) mouse model, salivary exosomes from patients with active IBD (active IBD-Sexos) exacerbated colitis, while those from IBD patients in remission (remission IBD-Sexos) did not. Possible reasons may include the regulation of macrophage polarization, disruption of intestinal epithelial function, and alteration of the intestinal flora. During co-culture with active IBD-Sexos, THP-1 cells exhibited inflammatory responses, while Caco-2 cells showed reduced tight junction protein expression. Additionally, 35 differentially expressed miRNAs were identified in active IBD-Sexos. In brief, our findings substantiate an intriguing phenomenon whereby active IBD-Sexos exacerbate colitis by bridging the oral cavity and intestine.

INTRODUCTION

Inflammatory bowel disease (IBD) is a lifelong disorder that impacts the rectum, colon, ileum, and the entire gastrointestinal tract. It includes two major forms: ulcerative colitis (UC) and crohn's disease (CD).[1] During the twenty-first century, IBD is a global healthcare problem with a consistently increasing incidence.[2,3] Although the exact mechanisms underlying the development of IBD remain unclear, the epithelial barrier function and the innate and adaptive immune systems are believed to play a significant role. Additionally, gut bacteria may contribute to the dysfunction of the intestinal immune system.[1,4,5]

Although the intestine is the main organ involved in IBD, as a systemic immune response disease, patients with IBD can have a combination of extraintestinal manifestations, and the mouth is noted as the most commonly involved extraintestinal location in active IBD patients.[6,7] On the other hand, the mouth is the initial segment of the gastrointestinal pathway, potentially reflecting or affecting the mucosa of the intestine to some degree.[7,8] Therefore, the question of whether and how the oral cavity affects intestinal inflammation has attracted increasing attention. The potential way underlying the oral contribution to colitis may involve two key aspects. Firstly, pathogenic bacteria in the oral cavity, such as *Porphyromonas gingivalis*, can compromise the integrity of the barrier between intestinal and epithelial tissues.[9] Secondly, oral-related immune cells can migrate to the intestine via the lymphatic pathway.[10] Although abundant reports exist, the exact reasons for these interactions are still incomplete. Therefore, this investigation aims to delve deeper into the intricate pathways involved in communication across intestinal compartments and the oral cavity.

As an easily collected bodily fluid, human saliva can be a strong reference for illness diagnosis.[11–14] Adults typically swallow 1.5 L of saliva daily, as food and microorganisms are mixed with saliva originating in the oral cavity into the gastrointestinal region. This suggests a potential connection between the oral cavity and IBD, with saliva acting as a mediator that promotes persistent chronic inflammation of the intestine.[9,14,15] Exosomes are microvesicles produced by varied cell types located across diverse body fluids, encompassing saliva and others, operating in information exchange, particularly for communication between distal organs.[16,17] Several studies have suggested that salivary exosomal contents have characteristic changes in various oral and systemic diseases, including pancreatic cancer, as well as Parkinson's and Alzheimer's diseases.[12,18–20] Nonetheless, the importance of salivary exosomal abnormalities in systemic diseases is still unclear. To date, it remains unelucidated whether salivary exosomes participate in intestinal inflammation.

In a previous investigation, we found that proteins specifically related to inflammation and immunity were increased in salivary exosomes from active IBD patients (IBD-Sexos) and hypothesized that salivary exosomes may reach the gut from the oral cavity, furthering IBD progression.[21] Our research has unveiled intriguing insights into the impact of the oral cavity on intestinal inflammation. Notably, we have discovered that salivary

[1]Department of Gastroenterology, Peking University People's Hospital, Beijing 100044, China
[2]Central Laboratory, Peking University School of Stomatology, Beijing 100081, China
[3]Center for Precision Medicine Multi-Omics Research, Institute of Advanced Clinical Medicine, Peking University, Beijing 100191, China
[4]Clinical Center of Immune-Mediated Digestive Diseases, Peking University People's Hospital, Beijing 100044, China
[5]Lead contact
*Correspondence: chenfeng2011@hsc.pku.edu.cn (F.C.), chenyang1816185048@bjmu.edu.cn (Y.C.), chenning79@bjmu.edu.cn (N.C.)
https://doi.org/10.1016/j.isci.2024.111061

Table 1. Testing cohort and clinical information

Description of study cohort	Total	UC	CD	Control
Total				
Patients (no %)	130,100%	58, 44.6%	47, 36.2%	25, 19.2%
Sex (f/m)	50/80	28/30	10/37	12/13
Age (mean +SD)	38.9 ± 13.8	45.6 ± 12.8	33.6 ± 13.2	33.0 ± 10.5
Clinical course (year, means +SD)	6.8 ± 6.9	5.9 ± 6.7	7.8 ± 7.1	–
Active$_a$				
Patients (no %)	62, 100	39, 62.9%	23, 37.1%	–
Sex (f/m)	28/30	19/20	9/10	–
Age (mean + SD)	41.3 ± 14.6	46.1 ± 13.7	33.3 ± 12.7	–
Clinical course (year, mean +SD)	6.3 ± 6.2	6.0 ± 6.2	6.7 ± 6.4	–
Mayo (mean + SD)	–	4.7 ± 1.6	–	–
CDAI (mean + SD)	–	–	200.7 ± 97.7	–
Serum (mean +SD)				
Patients (no.%)	52, 100%	29, 55.8%	23, 44.2%	–
CRP (mg/L)	11.8 ± 21.8	8.4 ± 17.6	16.2 ± 26.0	–
Patients (no.%)	48, 100%	25, 52.1%	23, 47.9%	–
ESR (mm/h)	24.9 ± 26.3	24.6 ± 29.2	25.3 ± 23.4	–
Remission				
Patients (no.%)	43	19,44.1%	24,55.9%	–
Sex (f/m)	13/30	9/10	4/20	–
Age (mean + SD)	38.7 ± 13.6	44.7 ± 10.9	34.0 ± 13.9	–
Clinical Course (year, mean + SD)	7.6 ± 7.9	5.8 ± 7.8	8.9 ± 7.8	–
Mayo (mean + SD)	–	1.3 ± 0.7	–	–
CDAI (mean + SD)	–	–	90.1 ± 43.0	–
Serum (mean + SD)				
Patients (no.%)	35, 100%	11, 31.4%	24, 68.6%	–
CRP (mg/L)	1.9 ± 2.1	2.2 ± 2.6	1.7 ± 1.9	–
Patients (no.%)	27, 100%	5, 18.5%	22, 81.5%	–
ESR (mm/h)	9.8 ± 5.8	12.7 ± 5.4	8.6 ± 5.7	–
Treatment				
Corticosteroids (no.%)	12, 100%	9, 75%	3, 25%	–
5-ASA (no.%)	40, 100%	36, 90.0%	4, 10.0%	–
Azathioprine	9, 100%	3, 33.3%	6, 66.7%	–
TNFα Inhibitor (no.%)	27, 100%	5, 18.5%	22, 81.5%	–
IL-12/23 Inhibitor (no.%)	10, 100%	2, 20.0%	8, 80.0%	–
Integrin Inhibitor (no.%)	12, 100%	10, 83.3%	2, 16.7%	–
Surgery (no.%)	10, 100%	2, 20.0%	8, 80.0%	–

For activity, remission was determined using CDAI <150 and CDEI <5 (CD), and Mayo score<3 (UC).

exosomes from patients with active IBD possess the capability to advance the progression of intestinal inflammation. Large amounts of saliva and salivary exosomes were generated continuously daily, indicating their impact on gut conditions is substantial. This study underscores the implications of the exosome-mediated oral-gut axis in gastrointestinal wellness and illness, providing insights into the pathogenesis of IBD.

RESULTS

Characterization of salivary exosomes

As presented in Tables 1 and S1, 105 patients with active IBD ($n = 62$, 39 UC and 23 CD, 28 females, and 30 males) or in remission ($n = 43$, 19 UC and 24 CD, 13 females, and 30 males) were included. The features and pureness of salivary exosomes were characterized through nanoparticle

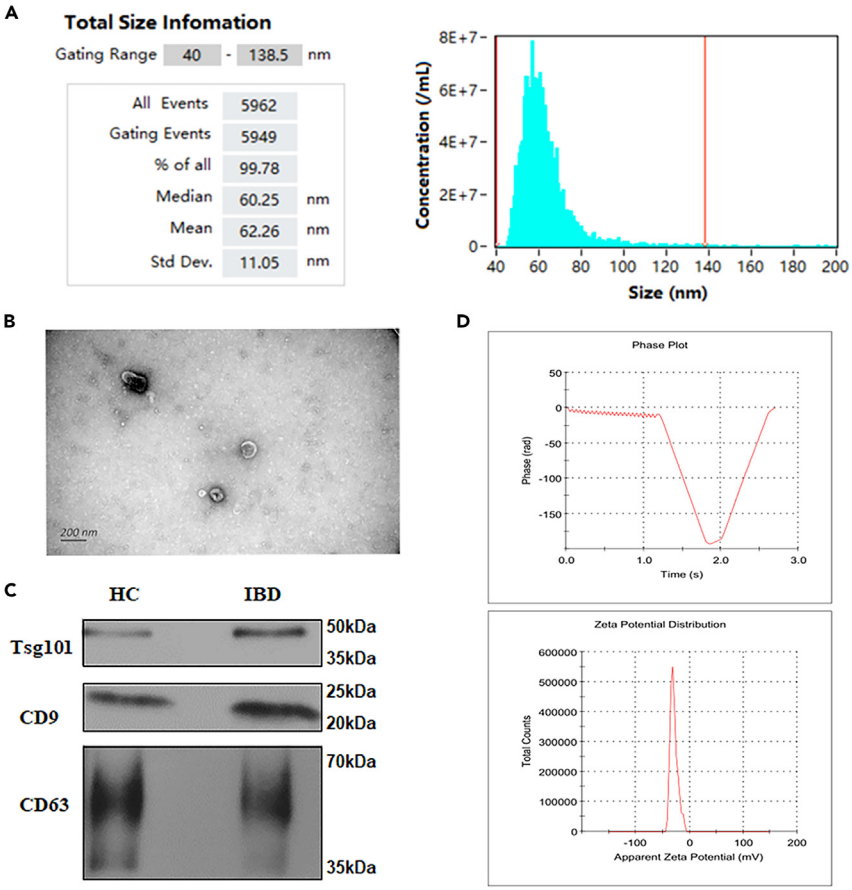

Figure 1. Isolation and characterization of salivary exosomes

(A) Size distribution and purify analysis of salivary exosomes by NTA.

(B) TEM photos of salivary exosomes. Scale bars: 200 nm.

(C) Salivary exosomes markers (Tsg101, CD9, CD63) analyzed with western blotting.

(D) Surface zeta potential (~−20 mV) of salivary exosomes.

tracing analysis (NTA), western blotting, and transmission electron microscopy (TEM). NTA results indicated that exosomes from saliva possessed a particle size of approximately 60 nm, mostly between 40 and 80 nm, which corresponded to the theoretical salivary exosome size (Figure 1A). TEM revealed that salivary exosomes exhibited a bilayer membrane structure and a saucer-like morphology (Figure 1B). Exosomal typical marker proteins CD9, CD63, and Tsg101 were all expressed in the western blot (Figure 1C). The surface zeta potential of salivary exosome is about −20 mV. (Figure 1D).

Salivary exosomes isolated from active IBD-Sexos exacerbate DSS-induced murine colitis, although salivary exosomes isolated from the remission IBD-Sexos do not

To examine the impact of salivary exosomes *in vivo*, mouse models were created, as illustrated in Figure 2A; mice were separated into 7 groups. Dextran sulfate sodium (DSS) mice were given PBS or salivary exosomes by gavage. Salivary exosomes were extracted from patients with active UC, remission UC, active CD, remission CD, and healthy control, respectively. First, we want to ensure that the exosomes can reach the intestine from the mouth. 1,1′-dioctadecyl-3,3,3′,3′-tetramethylindocarbocyanine perchlorate (DIL)-labeled salivary exosomes were administered to mice by gavage, and fluorescence images were taken 6 h later. As shown in Figure 2B, DIL-labeled salivary exosomes were mainly concentrated in the colon of mice at 6 h post-gavage, which suggested that salivary exosomes were able to expand to and collect in the colon via the "oral-gut axis" pathway. We observed that active IBD-Sexos aggravated weight reduction as well as colon length reduction in DSS mice, while remission IBD-Sexos did not exhibit proinflammatory effects (Figures 2C–2E). To gain deeper insights into the absorption of salivary exosomes by other organs, we assessed fluorescent signals in various organs of mice 24 h post-gavage. Notably, the signals primarily remained in the gastrointestinal tract, with no significant fluorescence observed in the liver, spleen, or kidneys (Figure S1). Furthermore, histological analysis showed that DSS mice gavaged with salivary exosomes isolated from patients with active UC and active CD had more severe mucosal damage, which manifested as severe bowel edema and large numbers of inflammatory cell infiltrations (Figures 2F, 2G, and S2).

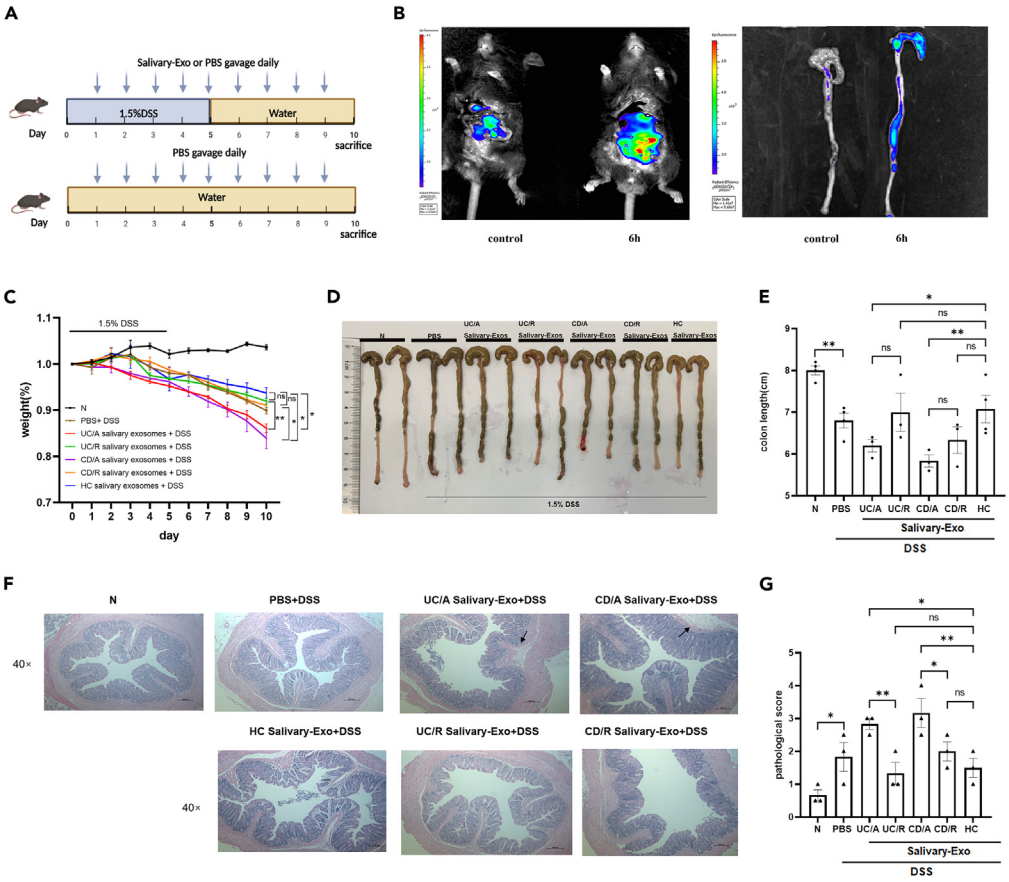

Figure 2. Salivary exosomes (Salivary-Exo) aggravate DSS-induced murine colitis

(A) A schematic diagram outlining the administration timeline of salivary exosomes in DSS-induced murine colitis. Mice are divided into seven groups.

(B) The fluorescence scattering of DIL-labeled salivary exosomes throughout the mouse colon following intragastric administration.

(C) Change in body mass among different treatment groups. UC/A vs. PBS: *, UC/R vs. PBS: ns, CD/A vs. PBS: *, CD/R vs. PBS: ns, healthy control (HC) vs. PBS: ns, PBS vs. N: ***.

(D and E) Colon-length contrast. UC/A vs. PBS: ns, UC/R vs. PBS: ns, CD/A vs. PBS: *, CD/R vs. PBS: ns, HC vs. PBS: ns.

(F and G) Representative colon segments were stained using H&E (scale bars: 200 μm). UC/A vs. PBS: *, UC/R vs. PBS: ns, CD/A vs. PBS: *, CD/R vs. PBS: ns, HC vs. PBS: ns. UC/A: UC in the active phase, UC/R: UC in remission, CD/A: CD in the active phase, CD/R: CD in remission, HC: healthy control. Data refer to means ± SEM. $N = 3$ to 4 mice per group. *$p < 0.05$, **$p < 0.01$.

In conclusion, the aforementioned results confirmed that salivary exosomes from patients during IBD flares indeed aggravate the colitis in the DSS mouse model, while remission IBD-Sexos does not. What is more, to elucidate the potential role of saliva as a vector for exosomes in the pathophysiology of IBD, saliva samples were collected from healthy individuals, active IBD patients, and IBD patients in remission, then administered to DSS-induced colitis mice. Changes in body weight and colon length were monitored. While saliva from IBD patients showed a trend toward worsening colonic inflammation compared to healthy controls, the effect was not statistically significant (Figure S3).

Effect of salivary exosomes on mucosal inflammation and intestinal barrier integrity

We used Caco-2 cells to assess the influence of salivary exosomes on the intestinal membrane. Caco-2 cells had inflammation encouraged using lipopolysaccharide (LPS), and they were co-cultured alongside salivary exosomes derived from IBD patients in different disease states (Figure 3A). The results revealed that salivary exosomes from active CD patients promoted inflammation in colonic epithelial cells, evidenced by increased interleukin (IL)-6, IL-1β, and tumor necrosis factor alpha (TNF-α) levels measured by ELISA. Likewise, exosomes from active UC patients raised TNF-α levels in these cells. In contrast, salivary exosomes from IBD patients in remission have no such effect (Figures 3C–3E). Western blotting analysis was employed to characterize the expression of zo-1 protein in Caco-2 monolayer cells under different treatment groups. The results showed that active IBD-Sexos could reduce zo-1 expression relative to the other classes (Figure 3B). However, in the absence of LPS stimulation, salivary exosomes have not demonstrated the capacity to elicit an inflammatory response in Caco-2 cells (Figure S4). To confirm the influence of salivary exosomes from IBD patients on intestinal epithelium *in vivo*, western blotting was utilized to identify the expressions of caspase-3 and zo-1 in each group. The results suggested a reduction in zo-1 levels in

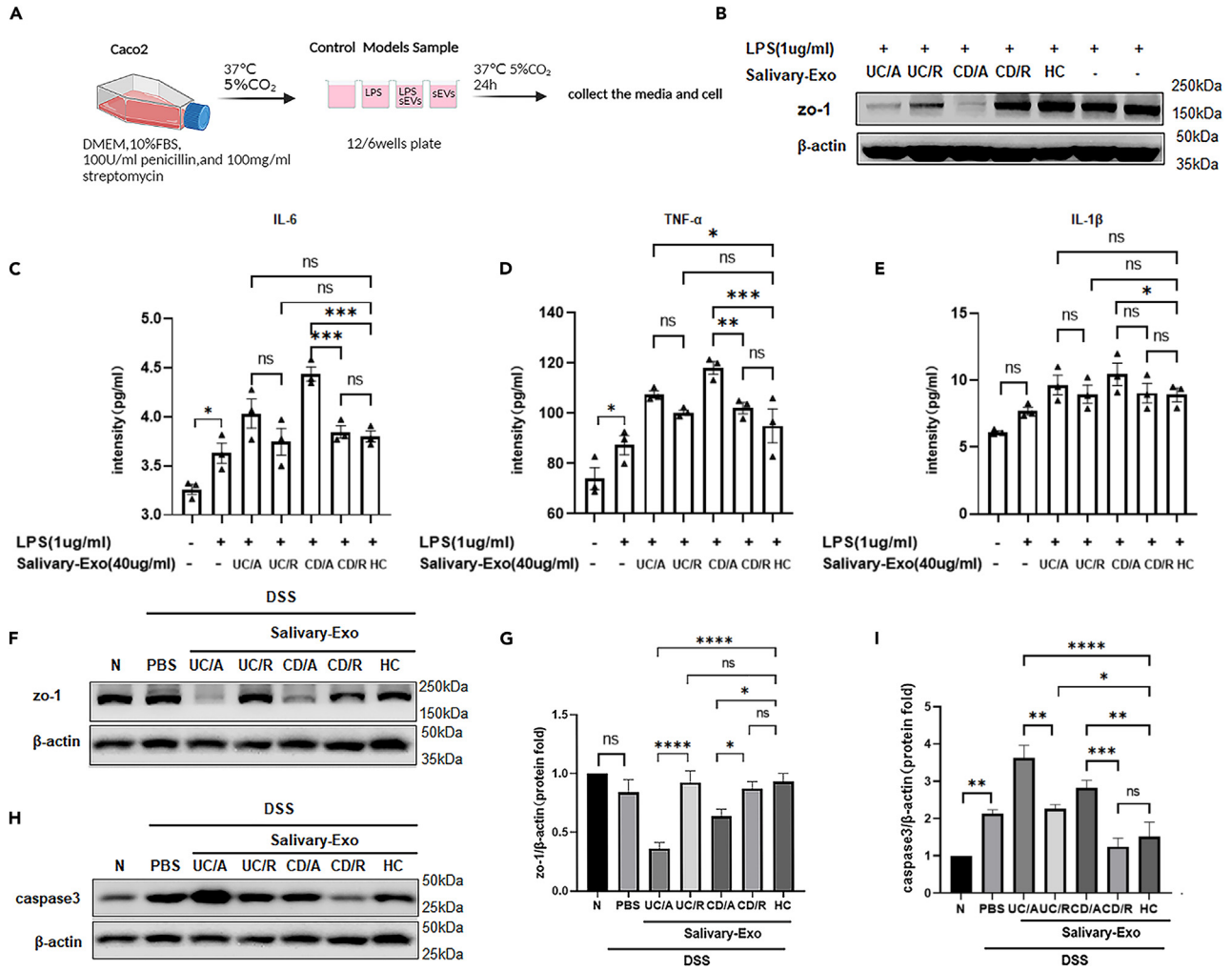

Figure 3. Effect of salivary exosomes on mucosal inflammation and intestinal barrier integrity

(A) Co-culture model of salivary exosomes and Caco-2 cells *in vitro*.

(B) The ZO-1 expression in Caco-2 cells was evaluated by western blot.

(C–E) Protein levels of cytokines IL-6, TNF-α, and IL-1β were assessed in the cell supernatant of Caco-2 cells using ELISA. IL-6: UC/A vs. LPS: *, UC/R vs. LPS: ns, CD/A vs. LPS: ****, CD/R vs. LPS: ns, HC vs. LPS: ns; TNF-α: UC/A vs. LPS: **, UC/R vs. LPS: *, CD/A vs. LPS: ****, CD/R vs. LPS: *, HC vs. LPS: ns; IL-1β: UC/A vs. LPS: *, UC/R vs. LPS: ns, CD/A vs. LPS: **, CD/R vs. LPS: ns, HC vs. LPS: ns.

(F and G) Representative western blotting of zo-1 DSS-induced mouse guts, and quantification of ZO-1 expression normalized to β-actin. UC/A vs. PBS: ***, UC/R vs. PBS: ns, CD/A vs. PBS: *, CD/R vs. PBS: ns, HC vs. PBS: ns.

(H and I) Western blot analysis of caspase-3 in the intestines of DSS mice, with quantification of caspase-3 protein expression levels standardized to β-actin. UC/A vs. PBS: ***, UC/R vs. PBS: ns, CD/A vs. PBS: *, CD/R vs. PBS: *, HC vs. PBS: ns. Data were presented as means ± SEM. ns: $p > 0.05$, *$p < 0.05$, **$p < 0.01$, ***$p < 0.001$.

the colons of DSS mice after administration of active IBD-Sexos (Figures 3F and 3G), and the intestinal epithelial cell apoptosis-related protein caspase-3 was increased in DSS mice following the gavage of salivary exosomes from UC patients in active phase (Figures 3H and 3I).

Active IBD-Sexos regulate gut immunity by remodeling macrophage phenotypes via upregulating the triggering of the NF-κB pathway

In order to examine the influence of salivary exosomes on the secretion of inflammatory features by macrophages, we differentiated THP-1 cells into macrophages using phorbol 12-myristate 13-acetate (PMA), followed by exposure to different groups of salivary exosomes for 24 h. Afterward, both the cells and the supernatant were collected. (Figure 4A). The findings from ELISA and real-time quantitative PCR (real-time qPCR) revealed that active IBD-Sexos induce inflammation in macrophages, resulting in heightened secretion of inflammatory cytokines

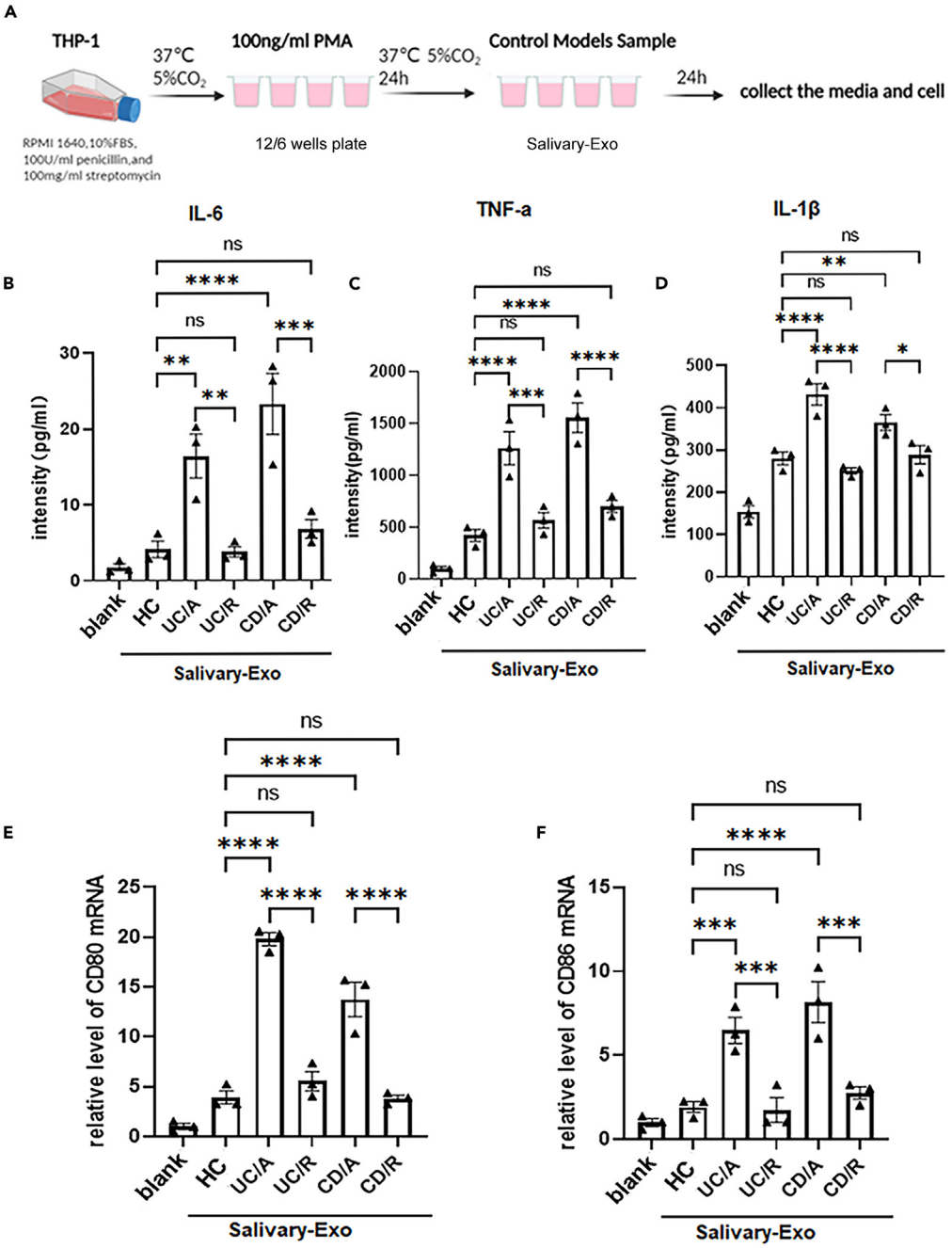

Figure 4. Impact of saliva-derived exosomes on THP-1 cells

(A) Co-culture model of salivary exosomes alongside THP-1 cells *in vitro*.

(B–D) Protein quantities of the cytokines IL-1β, IL-6, and TNF-α in the cell supernatant of THP-1 cells assessed via ELISA.

(E and F) mRNA levels of M1 macrophage makers CD80 and CD86 were measured using real-time qPCR (normalized to GAPDH). Data were presented as means ± SEM. ns: $p > 0.05$, *$p < 0.05$, **$p < 0.01$, ***$p < 0.001$.

including IL-1β, IL-6, and TNF-α, while also facilitating the polarization of macrophages toward the M1 phenotype. In contrast, salivary exosomes from IBD patients in remission and healthy control have no such effect (Figures 4B–4F).

To confirm the influence of salivary exosomes on intestinal macrophages *in vivo*, we observed changes in macrophages within the colonic lamina propria. Immunohistochemistry was used to detect the macrophage population in colon tissue, revealing a significant infiltration of $CD68^+$ macrophages into the intestinal lamina propria following gavage of active IBD-Sexos to DSS mice (Figures 5A and 5B). To further clarify

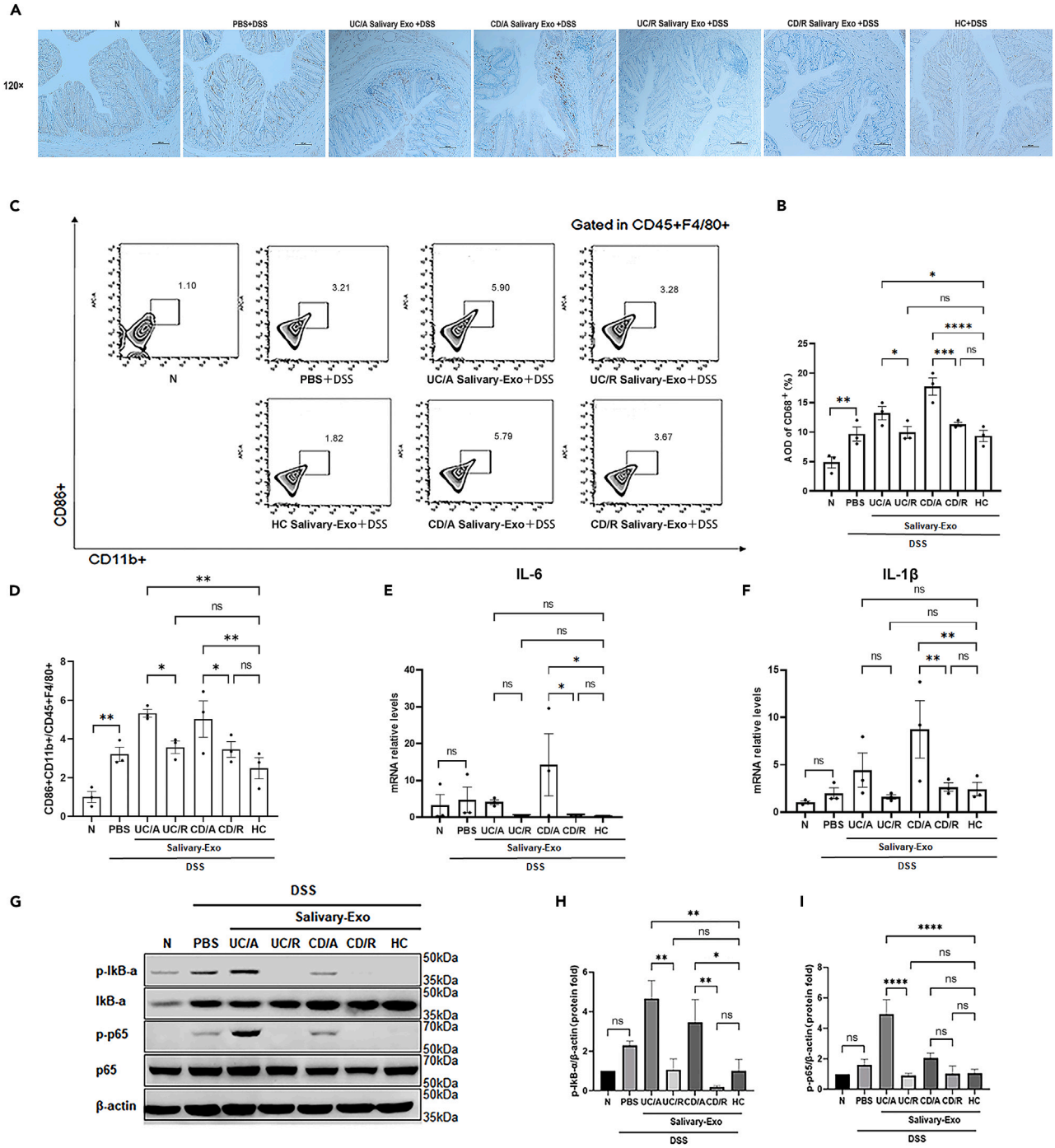

Figure 5. Salivary exosomes regulate gut immunity in DSS-induced mice via upregulating the initiation of the NF-κB pathway

(A and B) Expression of CD68+macrophages in colon tissue analyzed by immunohistochemistry (scale bars: 100 μm) and statistical examination. UC/A vs. PBS: *, UC/R vs. PBS: ns, CD/A vs. PBS: ****, CD/R vs. PBS: ns, HC vs. PBS: ns.

(C and D) Flow cytometry investigation of CD11b+ $CD86^+$ M1 macrophage cells and statistical analysis. UC/A vs. PBS: **, UC/R vs. PBS: ns, CD/A vs. PBS: *, CD/R vs. PBS: ns, HC vs. PBS: ns.

(E and F) mRNA levels of IL-1β and IL-6 in colon tissue (normalized to GAPDH). IL-6: CD/A vs. PBS: *; IL-1β: CD/A vs. PBS: **; no statistical significance observed in comparison of other groups with PBS.

(G–I) Representative western blotting of phosphorylated IκBα (p-IκBα), IκBα, p-p65, p65, and β-actin in the colon, quantification of the protein levels of p-p65 and p-IκBα, normalized to β-actin. p-IκBα: UC/A vs. PBS: *, UC/R vs. PBS: ns, CD/A vs. PBS: *, CD/R vs. PBS: *, HC vs. PBS: ns; p-p65: UC/A vs. PBS: ***, UC/R vs. PBS: ns, CD/A vs. PBS: ns, CD/R vs. PBS: ns, HC vs. PBS: ns. Data were presented as means ± SEM. ns: $p > 0.05$, *$p < 0.05$, **$p < 0.01$, ***$p < 0.001$.

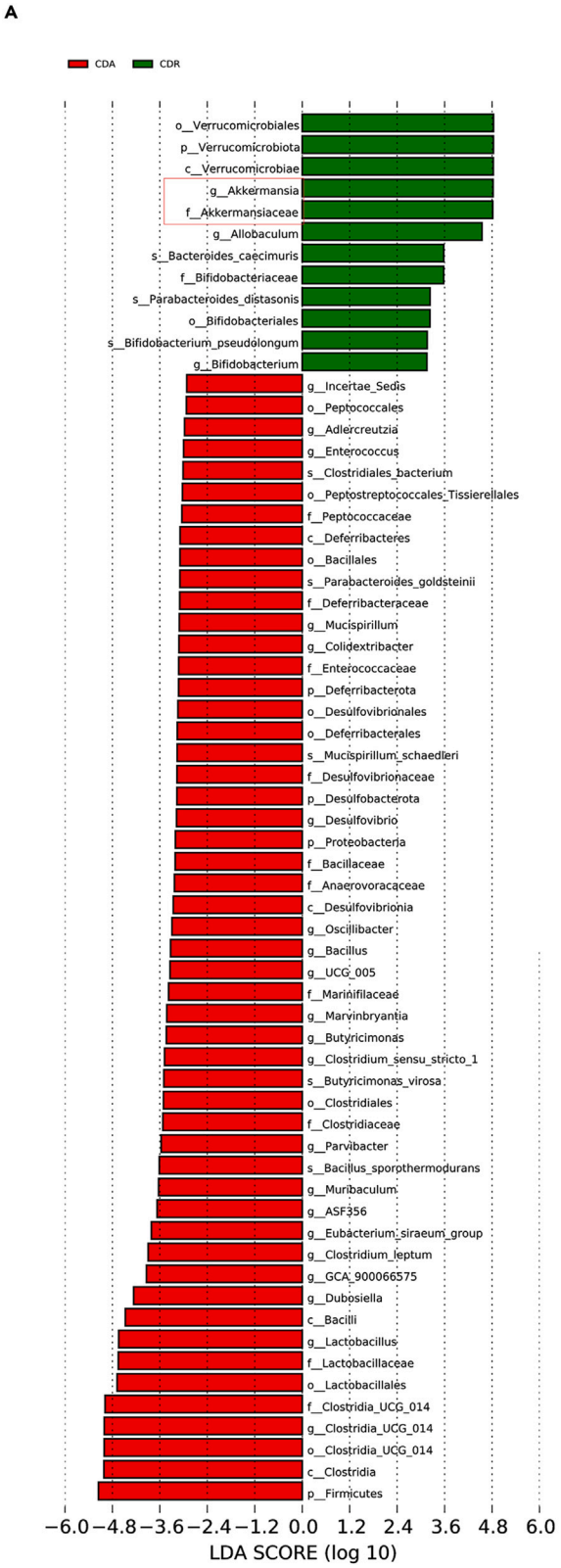
A
CDA
CDR
o__Verrucomicrobiales
p__Verrucomicrobiota
c__Verrucomicrobiae
g__Akkermansia
f__Akkermansiaceae
g__Allobaculum
s__Bacteroides_caecimuris
f__Bifidobacteriaceae
s__Parabacteroides_distasonis
o__Bifidobacteriales
s__Bifidobacterium_pseudolongum
g__Bifidobacterium
g__Incertae_Sedis
o__Peptococcales
g__Adlercreutzia
g__Enterococcus
s__Clostridiales_bacterium
o__Peptostreptococcales-Tissierellales
f__Peptococcaceae
c__Deferribacteres
o__Bacillales
s__Parabacteroides_goldsteinii
f__Deferribacteraceae
g__Mucispirillum
g__Colidextribacter
f__Enterococcaceae
p__Deferribacterota
o__Desulfovibrionales
o__Deferribacterales
s__Mucispirillum_schaedleri
f__Desulfovibrionaceae
p__Desulfobacterota
g__Desulfovibrio
p__Proteobacteria
f__Bacillaceae
f__Anaerovoracaceae
c__Desulfovibrionia
g__Oscillibacter
g__Bacillus
g__UCG_005
f__Marinifilaceae
g__Marvinbryantia
g__Butyricimonas
g__Clostridium_sensu_stricto_1
s__Butyricimonas_virosa
o__Clostridiales
f__Clostridiaceae
g__Parvibacter
s__Bacillus_sporothermodurans
g__Muribaculum
g__ASF356
g__Eubacterium_siraeum_group
g__Clostridium_leptum
g__GCA_900066575
g__Dubosiella
c__Bacilli
g__Lactobacillus
f__Lactobacillaceae
o__Lactobacillales
f__Clostridia_UCG_014
g__Clostridia_UCG_014
o__Clostridia_UCG_014
c__Clostridia
p__Firmicutes
−6.0 −4.8 −3.6 −2.4 −1.2 0.0 1.2 2.4 3.6 4.8 6.0
LDA SCORE (log 10)

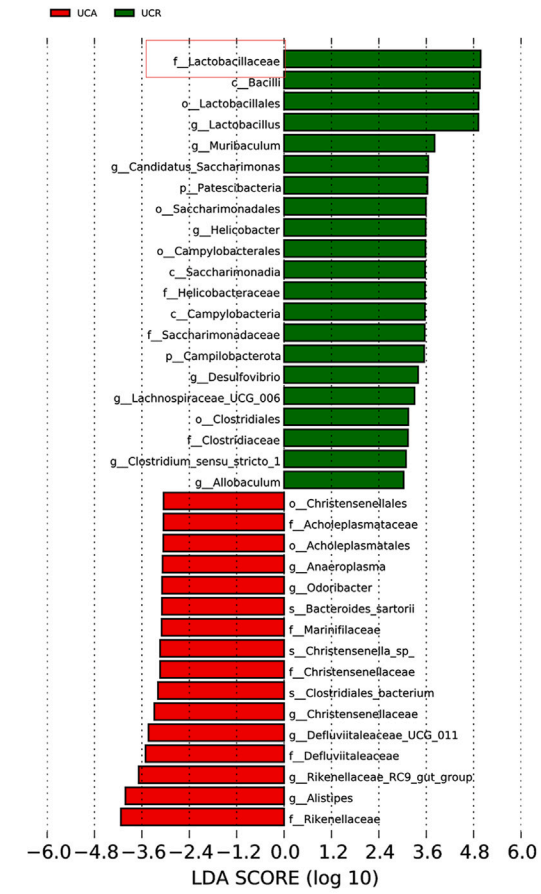
B
UCA
UCR
f__Lactobacillaceae
c__Bacilli
o__Lactobacillales
g__Lactobacillus
g__Muribaculum
g__Candidatus_Saccharimonas
p__Patescibacteria
o__Saccharimonadales
g__Helicobacter
o__Campylobacterales
c__Saccharimonadia
f__Helicobacteraceae
c__Campylobacteria
f__Saccharimonadaceae
p__Campilobacterota
g__Desulfovibrio
g__Lachnospiraceae_UCG_006
o__Clostridiales
f__Clostridiaceae
g__Clostridium_sensu_stricto_1
g__Allobaculum
o__Christensenellales
f__Acholeplasmataceae
o__Acholeplasmatales
g__Anaeroplasma
g__Odoribacter
s__Bacteroides_sartorii
f__Marinifilaceae
s__Christensenella_sp_
f__Christensenellaceae
s__Clostridiales_bacterium
g__Christensenellaceae
g__Defluviitaleaceae_UCG_011
f__Defluviitaleaceae
g__Rikenellaceae_RC9_gut_group
g__Alistipes
f__Rikenellaceae
−6.0 −4.8 −3.6 −2.4 −1.2 0.0 1.2 2.4 3.6 4.8 6.0
LDA SCORE (log 10)

Figure 6. Salivary exosomes reshape the gut microbiota configuration in DSS-induced mice

(A) The linear discriminant analysis (LDA) effect size (LEfSe) characterized the bacterial community between UC/A salivary Exo+ DSS and UC/R salivary Exo+ DSS at the genus level.

(B) LEfSe was utilized to assess the bacterial groupings between CD/A salivary Exo+ DSS and CD/R salivary Exo+ DSS at the genus level. An LDA score over three indicates a higher relative level in the associated group than others.

macrophage typing, we used flow cytometry to detect surface markers of M1-type macrophages. The findings indicated that an elevation in $CD86^{+}CD11b+$ macrophages was observed by flow cytometry, indicating an increase in M1 macrophages (Figures 5C, 5D, and S5). Then, we characterized the influence of salivary exosomes on inflammatory cytokine generation mechanistically associated with IBD. CD/A-Sexos administration increased the levels of several inflammatory cytokines, including IL-1β and IL-6 (Figures 5E and 5F). Then, we assessed the expression of various crucial regulators of the NF-κB signaling pathways using western blotting. The phosphorylation levels of IKBα and p65 were augmented significantly in DSS mice following the gavage of active IBD-Sexos (Figures 5G–5I). So, active IBD-Sexos make a difference in epithelial barrier function and intestinal immune dysfunction by degrading the IκB-α, which was the inhibitory protein of NF-κB, then the p65 translocated into the nucleus to trigger NF-κB signaling pathways.

Effect of salivary exosomes on the makeup of intestinal microbiota in DSS-induced mice

Intestinal microbiota imbalance critically influences the pathogenesis and development of IBD. After confirming the role of salivary exosomes in modulating intestinal immunity, we explored whether salivary exosomes could influence the gut microbiota. The results of the principal-component analysis based on the amplicon sequence variant level of the gut microbiota in mice from various groups are depicted in Figure S6A. Compared to the control group (N), significant alterations in the gut microbiota composition were observed in the remaining six groups of mice with colitis. Notably, the group treated with CD/A-Sexos exhibited the most pronounced changes in the gut microbiota community structure. What's more, we investigated the fecal material of mice in each group by 16S rRNA sequencing. LEfSe (LDA effect size) can find the biomarker with statistical differences between groups. The results demonstrated an elevated abundance of *Lactobacillus* in DSS-induced colitis mice after the gavage of salivary exosomes from UC patients in remission. Additionally, the proportion of *Akkermansia* showed a significant increase in DSS mice following the gavage of salivary exosomes obtained from CD patients in remission. On the contrary, in the DSS mice gavaged with active IBD-Sexos, although there was a compensatory increase in the proportion of probiotics, there was also an elevation in the levels of damaging bacteria like *Enterococcus* and *Clostridium* (Figures 6A, 6B, S6B, and S6C). These findings suggested that salivary exosomes may function in regulating intestinal microbiota. Moreover, the regulatory effects of salivary exosomes from IBD patients with different disease states are not exactly the same.

Salivary exosome microRNAs differ between the stages of IBD

To identify the immune regulatory approaches applied by salivary exosomes in the DSS-induced colitis model, our previous bioinformatics data showed that proteins related to immune signaling pathways in the salivary exosomes from IBD patients in the active phase (Figure S7). Moreover, we explored the immunoregulatory functions of salivary exosomes by conducting microRNA profile analysis on salivary exosomes derived from patients with active IBD, IBD patients in remission, and healthy control. We identified 35 differentially expressed microRNAs in active IBD-Sexos compared to exosomes extracted from IBD patients in remission and healthy control, indicating a unique immune and inflammatory signature associated with active IBD (Figures 7A and 7B). In particular, the expression of 29 microRNAs was significantly increased in active IBD patients' salivary exosomes including miR-223–3p, miR-119b-5p, miR-203–5p, etc. Moreover, to reveal the putative function of the salivary exosome augmented fractions isolated miRNA up- or downregulated in IBD individuals with different disease states, we investigated the possible influence of diverse miRNA on protein-coding mRNAs. Examining the bioinformatics miRNA target database revealed that targeted mRNAs were primarily increased in tight junction, apoptosis, and NF-κB pathways (Figure 7C). miR-223 serves as a fresh intermediary for the interaction between the IL23 signaling pathway and CLDN8, which causes the lack of effectiveness of the intestinal barrier and encourages IBD.[22] miR-119b-5p and miR-203–5p may function in the NF-κB signaling pathway. Additionally, we have analyzed the microRNA content variations in saliva-derived exosomes between active and remission phase IBD patients. We identified 15 microRNAs with altered expression in exosomes from active IBD patients versus those in remission. Notably, 11 were significantly upregulated in the exosomes of active IBD patients (Figures S8A and S8B). A bioinformatics analysis of miRNA target databases reveals that these microRNAs predominantly target mRNAs involved in crucial biological processes, including the tight junctions, focal adhesion, regulation of actin cytoskeleton, PI3K-Akt signaling pathway, cytokine-cytokine receptor interaction and oxidative phosphorylation, similar to active IBD vs. remission IBD and HC. Furthermore, these microRNAs target mRNAs that play roles in ubiquitination-mediated proteolysis (Figure S8C).

DISCUSSION

IBD is marked by relapsing and remission, necessitating long-term treatment for disease control.[23] Hence, an in-depth investigation into the pathogenesis of this condition holds particular significance, particularly in elucidating the mechanisms underlying recurrent intestinal inflammation in IBD. Oral microenvironment dysregulation may be implicated in the chronic inflammation of the intestinal tract in IBD.[8,10,24,25] Prior research has indicated alterations in salivary exosomes in both oral and systemic ailments.[18,19,26–30] Nonetheless, the significance of the mediated pathways in the pathogenesis of IBD induced by salivary exosomes remains unclear. This study unearthed that salivary exosomes from

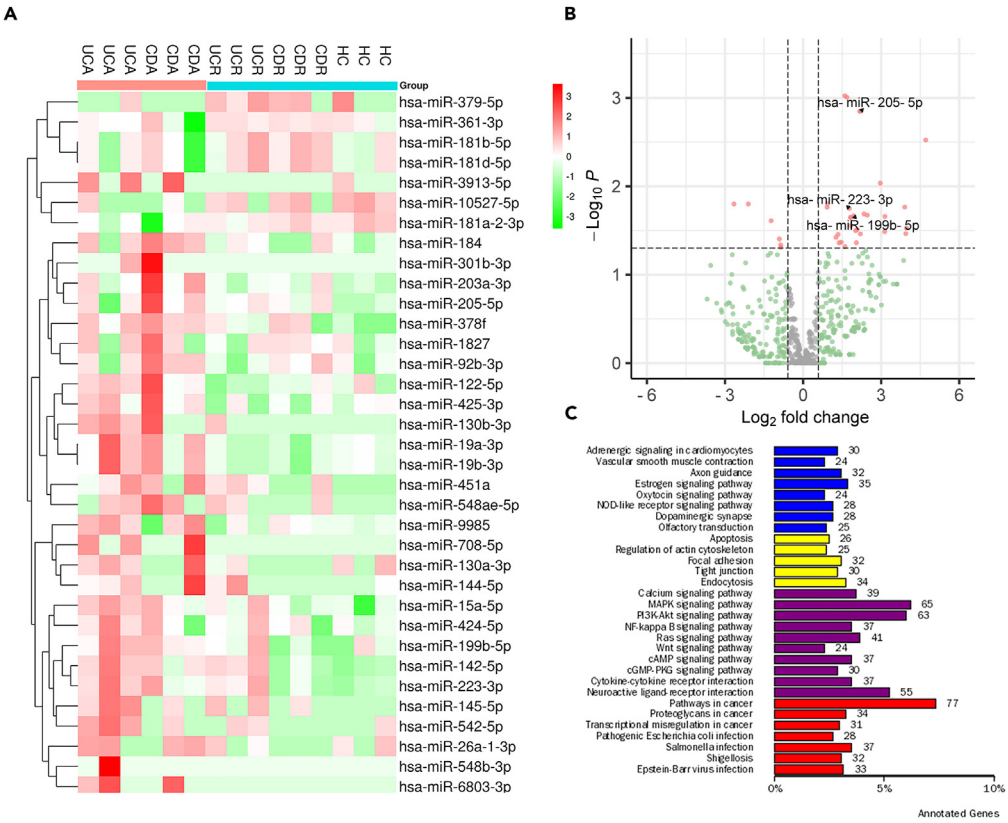

Figure 7. microRNAs contents of salivary exosomes from IBD patients with different stages

(A) A heatmap for altered microRNA content of salivary exosomes during IBD patients in the active phase.

(B) Volcano plot showing the diverse microRNA. (log2FC > 1.5, $p < 0.05$).

(C) A bar plot depicting the differentially expressed microRNAs targeting gene numbers across all Kyoto Encyclopedia of Genes and Genomes (KEGG) pathways.

active IBD patients harbor diverse substances that potentiate inflammation and immune responses, thereby fostering the progression of intestinal inflammation. Conversely, this effect was absent in salivary exosomes isolated from IBD patients in remission and controls. Furthermore, we also conducted preliminary explorations into the potential factors that contribute to this phenomenon (Figure 8).

Several investigations have indicated that "oral-gut axis" might be implicated in diverse intestinal and systemic disorder progression.[31] Oral microbiota triggers IBD progression. Research has found that oral microbiota in saliva can transit to the digestive tract through swallowing and interact with the microbial community in the intestines.[25] Some investigations have indicated that alterations in specific oral microbiota are associated with the onset and severity of IBD.[32] Atarashi et al. revealed that oral provision of saliva from IBD patients led to the colonization of potential oral pathogens in the intestines of mice, which may enhance intestinal inflammation, indicating that oral microbiota may operate as a "reservoir" of pathogenic bacteria linked to the development of IBD via the oral-gut axis.[33] Our previous research has shown that during periodontitis, there are changes in oral mucosal immune cells, which may exacerbate the intestinal inflammation in IBD.[34] However, while research on the involvement of saliva as a carrier of oral microbiota in IBD development is ongoing, there is still some controversy over the specific mechanisms involved, and further examination is required to validate and explain these findings. Therefore, there is a pressing need for more in-depth studies to elucidate the intricate role played by the oral-gut axis in the pathogenesis and progression of IBD.[31,35–37] In our study, we found that in addition to microorganisms, salivary exosomes, another substance in saliva that should not be ignored, are also involved in intestinal inflammation in IBD. Exosomes have the hallmarks of stable, long-distance transmission without disruption, and they are the primary players in material communication between distant cells.[16,38–40] Here, we established that salivary exosomes possess a critical role in interactions between the oral cavity and intestinal tract, aside from microorganisms or immune cells, exacerbating intestinal inflammation observed in IBD.

Currently, research on salivary exosomes typically entails utilizing them solely as biological markers to diagnose or monitor disease activity.[12,41] However, salivary exosomes are not only useful as biomarkers but may also hold profound significance in systemic ailments. Since exosomes do not cause immune rejection,[42] we produced a DSS mouse model to evaluate the function of salivary exosomes from patients with IBD. The findings of our research proved that salivary exosomes from patients during IBD flare-ups had a significant pro-inflammatory effect. In contrast, salivary exosomes extracted from remission IBD patients did not. While previous studies have posited that various transient stimuli may impact intestinal inflammation, the factors that create sustained inflammation remain unclear. Salivary exosomes can

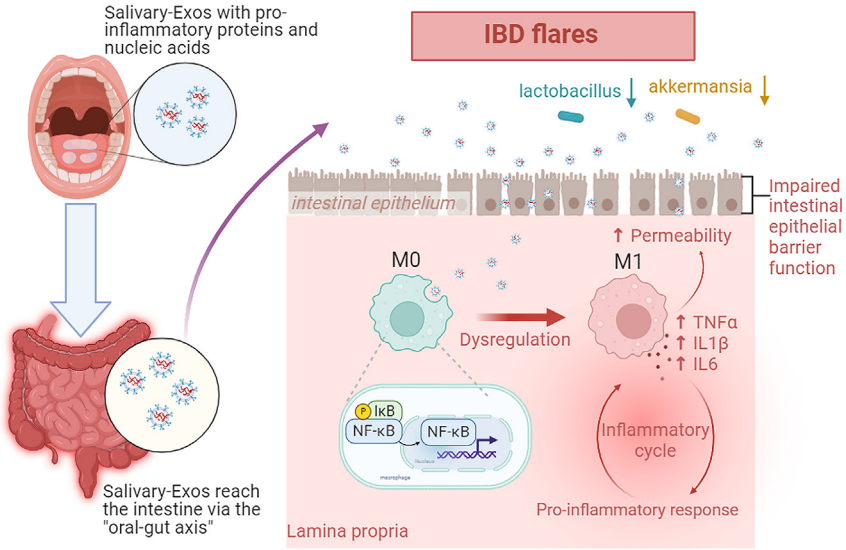

Figure 8. The model of salivary exosomes from patients during IBD flare-ups promoted intestinal inflammation

reach the intestines in a steady stream by swallowing saliva, leading to consistent stimulation of the intestines. Adults swallow about 1.5 L of saliva per day, IBD flare may last anywhere from a few weeks to several months, and salivary exosomes from IBD patients with active phase may be associated with chronic persistent intestinal inflammation. This research indicates that there are specific components or signaling molecules in the salivary exosomes of active IBD patients that promote colonic inflammation, which may lead to a worsening of inflammatory reactions. However, in remission, IBD patients and healthy control groups, salivary exosomes do not have such an effect. As for the specific processes by which saliva exosomes exacerbate intestinal inflammation in active IBD patients, further investigation is warranted to elucidate.

The activation and polarization of macrophages, as well as the regulation of intestinal permeability by TJ protein, have a critical role in IBD development. Numerous investigations have indicated that exosomes of different origins can act on the intestinal tract through circulation and may exert regulatory influence in IBD.[42] Liu L et al. observed that *Fusobacterium nucleatum* secreted extracellular vesicles that promote disruption of the intestinal membrane via initiation of the RIPK1-mediated pathway.[43] Another research reported that co-culturing THP-1 cells with exosomes derived from human umbilical cord mesenchymal stem cells *in vitro* caused increased cell survival to prove that the exosomes weaken colitis by modulating macrophages.[44] *In vitro*, the possible effect involved utilizing the Caco-2 cells model triggered by LPS to evaluate the pro-inflammation and intestinal obstacle disruption potential of salivary exosomes. THP-1 cells as a model for mimicking the function and regulation of salivary exosomes on macrophages. Interestingly, we observed that salivary exosomes alone did not appear to induce inflammation in Caco-2 cells in the absence of LPS stimulation. However, they did trigger the release of inflammatory cytokines in THP-1 cells. Given the minuscule size of exosomes, which allows for their passage through various biological barriers,[45] we hypothesize that upon reaching the gastrointestinal tract, salivary exosomes may traverse the intestinal epithelial barrier and interact with the lamina propria. There, they could stimulate resident macrophages to differentiate into the M1 phenotype and secrete inflammatory cytokines. This process may disrupt the tight junctions of the intestinal epithelium, resulting in a pro-inflammatory environment. *In vivo*, the potential effect of active IBD-Sexos is evidenced by the promotion of macrophage M1 polarization and disruption of zo-1 protein expression within the colons of mice induced with DSS.

Numerous studies suggested that perturbation of the balance between host and gut microbes produces immune inflammation in susceptible populations.[46–49] *Lactobacillus*-based therapy is a potentially effective treatment for chemokine-mediated diseases, including IBD, and *Akkermansia* has been shown to be able to regulate immune disorders in mice with colitis.[50–53] We found that salivary exosomes derived from IBD patients in remission leads to an elevated prevalence of beneficial gut microbes, such as *Lactobacillus* and *Akkermansia*. A study has demonstrated that administering intestinal exosomes derived from the healing stage orally was a practical method for curing specific cases of UC.[54] Consistent with previous research, our study suggested that the difference in microbiome, especially *Lactobacillus* and *Akkermansia* comparing treatment of salivary exosomes from patients in active or remission of IBD may potentially contribute to the mice phenotypes observed in the study.

Studies have shown that the composition of exosomes is influenced by both their generation pathway and physiological state.[55] Mitsuhashi et al. compared the exosomes present in the intestinal region of individuals with IBD to controls and identified significant differences in both mRNA and protein profiles across both groups.[56] In our study, we propose that the differential functional properties observed between active IBD-Sexos and remission IBD-Sexos may be attributed to certain pro-inflammatory substances present in the exosomes from the saliva of patients facing active IBD. These substances have the potential to be transported to the intestine through the "oral-gut axis," contributing to the continual progression of intestinal inflammation. Furthermore, identifying specific components within salivary exosomes that exert

bioactivity remains challenging. Our previous research has demonstrated that proteins found in the salivary exosomes of patients during IBD flare-ups play a crucial role in immunity and inflammation.[21] Additionally, through microRNA analysis of salivary exosomes, we have observed distinct variations in nucleic acid content among IBD patients with different disease states, suggesting that these molecules play diverse biological roles. Notably, immune and inflammatory activities appear to be distinctive features of salivary exosomes derived from active IBD patients. Thus, we suggest that the specific proteins and microRNAs in salivary exosomes from IBD patients work together to promote inflammation. Moreover, identifying the contents of salivary exosomes may be a crucial strategy for diagnosing IBD and assessing its activity. However, the exact proinflammatory components of salivary exosomes remain unknown and deserve further examination.

In summary, our data substantiate an intriguing phenomenon whereby salivary exosomes serve as mediators in the communication between the oral cavity and the gastrointestinal tract. Salivary exosomes isolated from patients during IBD flares can aggravate intestinal inflammation by disturbing the intestinal epithelial membrane, producing immune dysregulation within the intestinal lamina propria, and controlling the gut microbiota configuration. In contrast, salivary exosomes isolated from IBD patients in remission and normal individuals do not demonstrate such effects. This study elucidated the function of exosomes from saliva in IBD, thereby bolstering our understanding of the oral-gut axis. Additionally, future exploration may delve into the roles and mechanisms of specific proteins or nucleic acids within salivary exosomes. This study offers fresh perspectives on the pathogenesis of IBD and lays the groundwork for further examination of the potential pathophysiological functions of salivary exosomes. Furthermore, saliva may be easily obtained multiple times within a short time frame, making it a promising avenue for future IBD diagnosis and drug efficacy prediction research.

Limitations of the study

The specific proteins and microRNAs in salivary exosomes from IBD patients work together to promote inflammation. However, the exact proinflammatory components of salivary exosomes remain unknown in this study and deserve further examination.

RESOURCE AVAILABILITY

Lead contact

Further information and requests for resources and reagents should be directed to and will be fulfilled by the corresponding author, Professor Ning Chen (chenning79@bjmu.edu.cn).

Materials availability

This work did not generate new unique reagents. Primers sequences used are provided in Table S2, and available upon request to the corresponding author.

Data and code availability

The raw sequence data reported in this paper have been deposited in the Genome Sequence Archive (Genomics, Proteomics & Bioinformatics 2021) in National Genomics Data Center (Nucleic Acids Res 2021), China National Center for Bioinformation/Beijing Institute of Genomics, Chinese Academy of Sciences. "GSA: CRA017599" is publicly accessible at https://ngdc.cncb.ac.cn/gsa. "GSA-Human: HRA007892" can be accessed upon request through https://ngdc.cncb.ac.cn/gsa-human/. The data reported in this paper will be shared upon request to the lead corresponding author (chenning79@bjmu.edu.cn). This paper dose not report original code. Any additional information required to reanalyze the data reported in this paper is available from the lead contact upon request.

ACKNOWLEDGMENTS

The authors disclosed receipt of the following financial support for the research, authorship, and/or publication of this article: The work was supported by grants from the National Natural Science Foundation of China (Nos. 82070566), Clinical Medicine Plus X-Young Scholars Project of Peking University (PKU2023LCXQ027), Peking University People's Hospital Research And Development Funds (RDGS2022-09), the KCL and PKUHSC Joint Institute for Medical Research Fund (BMU2020KCL003), National Key Research and Development Program of China (2022YFA1206103), Research Funds from the Health@InnoHK Program launched by the Innovation Technology Commission of the Hong Kong Special Administrative Region.

AUTHOR CONTRIBUTIONS

C.Y.: sample collection, methodology, project administration, validation, writing – original draft. J.C: project administration, investigation, methodology. Y.Z.: sample collection, validation, visualization. J.W. and Y.X.: sample collection, methodology. J.X.: methodology, supervision. F.C.: methodology, resources, supervision, funding acquisition. Y.C.: formal analysis, funding acquisition, investigation, writing – review and editing. N.C.: conceptualization, data curation, formal analysis, funding acquisition, investigation, resources, supervision, writing – review and editing.

DECLARATION OF INTERESTS

The authors declare no competing interests.

STAR★METHODS

Detailed methods are provided in the online version of this paper and include the following:

- KEY RESOURCES TABLE
- EXPERIMENTAL MODEL AND STUDY PARTICIPANT DETAILS
  - Ethics approval and consent to participate
  - Animal model and treatment
  - Cell culturing

SUPPLEMENTAL INFORMATION

Supplemental information can be found online at https://doi.org/10.1016/j.isci.2024.111061.

Received: May 24, 2024
Revised: July 18, 2024
Accepted: September 24, 2024
Published: September 27, 2024

REFERENCES

1. Xavier, R.J., and Podolsky, D.K. (2007). Unravelling the pathogenesis of inflammatory bowel disease. Nature *448*, 427–434. https://doi.org/10.1038/nature06005.
2. Ng, S.C., Shi, H.Y., Hamidi, N., Underwood, F.E., Tang, W., Benchimol, E.I., Panaccione, R., Ghosh, S., Wu, J.C.Y., Chan, F.K.L., et al. (2017). Worldwide incidence and prevalence of inflammatory bowel disease in the 21st century: a systematic review of population-based studies. Lancet (London, England) *390*, 2769–2778. https://doi.org/10.1016/s0140-6736(17)32448-0.
3. Kaplan, G.G. (2015). The global burden of IBD: from 2015 to 2025. Nat. Rev. Gastroenterol. Hepatol. *12*, 720–727. https://doi.org/10.1038/nrgastro.2015.150.
4. Nell, S., Suerbaum, S., and Josenhans, C. (2010). The impact of the microbiota on the pathogenesis of IBD: lessons from mouse infection models. Nat. Rev. Microbiol. *8*, 564–577. https://doi.org/10.1038/nrmicro2403.
5. Li, J., Song, J., Deng, Z., Yang, J., Wang, X., Gao, B., Zhu, Y., Yang, M., Long, D., Luo, X., et al. (2024). Robust reactive oxygen species modulator hitchhiking yeast microcapsules for colitis alleviation by trilogically intestinal microenvironment renovation. Bioact. Mater. *36*, 203–220. https://doi.org/10.1016/j.bioactmat.2024.02.033.
6. Rogler, G., Singh, A., Kavanaugh, A., and Rubin, D.T. (2021). Extraintestinal Manifestations of Inflammatory Bowel Disease: Current Concepts, Treatment, and Implications for Disease Management. Gastroenterology *161*, 1118–1132. https://doi.org/10.1053/j.gastro.2021.07.042.
7. Lourenço, S.V., Hussein, T.P., Bologna, S.B., Sipahi, A.M., and Nico, M.M.S. (2010). Oral manifestations of inflammatory bowel disease: a review based on the observation of six cases. J. Eur. Acad. Dermatol. Venereol. *24*, 204–207. https://doi.org/10.1111/j.1468-3083.2009.03304.x.
8. Ray, K. (2020). The oral-gut axis in IBD. Nat. Rev. Gastroenterol. Hepatol. *17*, 532. https://doi.org/10.1038/s41575-020-0346-0.
9. Qian, J., Lu, J., Huang, Y., Wang, M., Chen, B., Bao, J., Wang, L., Cui, D., Luo, B., and Yan, F. (2022). Periodontitis Salivary Microbiota Worsens Colitis. J. Dent. Res. *101*, 559–568. https://doi.org/10.1177/00220345211049781.
10. Kitamoto, S., Nagao-Kitamoto, H., Jiao, Y., Gillilland, M.G., 3rd, Hayashi, A., Imai, J., Sugihara, K., Miyoshi, M., Brazil, J.C., Kuffa, P., et al. (2020). The Intermucosal Connection between the Mouth and Gut in Commensal Pathobiont-Driven Colitis. Cell *182*, 447–462.e14. https://doi.org/10.1016/j.cell.2020.05.048.
11. Gao, X., Jiang, S., Koh, D., and Hsu, C.Y.S. (2016). Salivary biomarkers for dental caries. Periodontology *70*, 128–141. https://doi.org/10.1111/prd.12100.
12. Han, Y., Jia, L., Zheng, Y., and Li, W. (2018). Salivary Exosomes: Emerging Roles in Systemic Disease. Int. J. Biol. Sci. *14*, 633–643. https://doi.org/10.7150/ijbs.25018.
13. Goldoni, R., Dolci, C., Boccalari, E., Inchingolo, F., Paghi, A., Strambini, L., Galimberti, D., and Tartaglia, G.M. (2022). Salivary biomarkers of neurodegenerative and demyelinating diseases and biosensors for their detection. Ageing Res. Rev. *76*, 101587. https://doi.org/10.1016/j.arr.2022.101587.
14. de Vries, S.A.G., Tan, C.X.W., Bouma, G., Forouzanfar, T., Brand, H.S., and de Boer, N.K. (2018). Salivary Function and Oral Health Problems in Crohn's Disease Patients. Inflamm. Bowel Dis. *24*, 1361–1367. https://doi.org/10.1093/ibd/izy017.
15. Bao, J., Li, L., Zhang, Y., Wang, M., Chen, F., Ge, S., Chen, B., and Yan, F. (2022). Periodontitis may induce gut microbiota dysbiosis via salivary microbiota. Int. J. Oral Sci. *14*, 32. https://doi.org/10.1038/s41368-022-00183-3.
16. Kalluri, R., and LeBleu, V.S. (2020). The biology, function, and biomedical applications of exosomes. Science (New York, NY) *367*, eaau6977. https://doi.org/10.1126/science.aau6977.
17. Jiang, J., Mei, J., Ma, Y., Jiang, S., Zhang, J., Yi, S., Feng, C., Liu, Y., and Liu, Y. (2022). Tumor hijacks macrophages and microbiota through extracellular vesicles. Exploration (Beijing, China) *2*, 20210144. https://doi.org/10.1002/exp.20210144.
18. Sun, Y., Huo, C., Qiao, Z., Shang, Z., Uzzaman, A., Liu, S., Jiang, X., Fan, L.Y., Ji, L., Guan, X., et al. (2018). Comparative Proteomic Analysis of Exosomes and Microvesicles in Human Saliva for Lung Cancer. J. Proteome Res. *17*, 1101–1107. https://doi.org/10.1021/acs.jproteome.7b00770.
19. Byun, J.S., Hong, S.H., Choi, J.K., Jung, J.K., and Lee, H.J. (2015). Diagnostic profiling of salivary exosomal microRNAs in oral lichen planus patients. Oral Dis. *21*, 987–993. https://doi.org/10.1111/odi.12374.
20. He, L., Ping, F., Fan, Z., Zhang, C., Deng, M., Cheng, B., and Xia, J. (2020). Salivary exosomal miR-24-3p serves as a potential detective biomarker for oral squamous cell carcinoma screening. Biomedicine & pharmacotherapy = Biomedecine & pharmacotherapie *121*, 109553. https://doi.org/10.1016/j.biopha.2019.109553.
21. Zheng, X., Chen, F., Zhang, Q., Liu, Y., You, P., Sun, S., Lin, J., and Chen, N. (2017). Salivary exosomal PSMA7: a promising biomarker of inflammatory bowel disease. Protein Cell *8*, 686–695. https://doi.org/10.1007/s13238-017-0413-7.
22. Wang, H., Chao, K., Ng, S.C., Bai, A.H., Yu, Q., Yu, J., Li, M., Cui, Y., Chen, M., Hu, J.F., and Zhang, S. (2016). Pro-inflammatory miR-223 mediates the cross-talk between the IL23 pathway and the intestinal barrier in inflammatory bowel disease. Genome Biol. *17*, 58. https://doi.org/10.1186/s13059-016-0901-8.
23. Chu, H., Khosravi, A., Kusumawardhani, I.P., Kwon, A.H.K., Vasconcelos, A.C., Cunha, L.D., Mayer, A.E., Shen, Y., Wu, W.L., Kambal, A., et al. (2016). Gene-microbiota interactions contribute to the pathogenesis of inflammatory bowel disease. Science (New York, NY) *352*, 1116–1120. https://doi.org/10.1126/science.aad9948.
24. Kobayashi, R., Ogawa, Y., Hashizume-Takizawa, T., and Kurita-Ochiai, T. (2020). Oral bacteria affect the gut microbiome and intestinal immunity. Pathog. Dis. *78*, ftaa024. https://doi.org/10.1093/femspd/ftaa024.
25. Byrd, K.M., and Gulati, A.S. (2021). The "Gum-Gut" Axis in Inflammatory Bowel Diseases: A Hypothesis-Driven Review of Associations

and Advances. Front. Immunol. *12*, 620124. https://doi.org/10.3389/fimmu.2021.620124.
26. Han, P., Lai, A., Salomon, C., and Ivanovski, S. (2020). Detection of Salivary Small Extracellular Vesicles Associated Inflammatory Cytokines Gene Methylation in Gingivitis. Int. J. Mol. Sci. *21*, 5273. https://doi.org/10.3390/ijms21155273.
27. Lin, Y., Dong, H., Deng, W., Lin, W., Li, K., Xiong, X., Guo, Y., Zhou, F., Ma, C., Chen, Y., et al. (2019). Evaluation of Salivary Exosomal Chimeric GOLM1-NAA35 RNA as a Potential Biomarker in Esophageal Carcinoma. Clin. Cancer Res. *25*, 3035–3045. https://doi.org/10.1158/1078-0432.Ccr-18-3169.
28. Winck, F.V., Prado Ribeiro, A.C., Ramos Domingues, R., Ling, L.Y., Riaño-Pachón, D.M., Rivera, C., Brandão, T.B., Gouvea, A.F., Santos-Silva, A.R., Coletta, R.D., and Paes Leme, A.F. (2015). Insights into immune responses in oral cancer through proteomic analysis of saliva and salivary extracellular vesicles. Sci. Rep. *5*, 16305. https://doi.org/10.1038/srep16305.
29. Mi, B., Chen, L., Xiong, Y., Yan, C., Xue, H., Panayi, A.C., Liu, J., Hu, L., Hu, Y., Cao, F., et al. (2020). Saliva exosomes-derived UBE2O mRNA promotes angiogenesis in cutaneous wounds by targeting SMAD6. J. Nanobiotechnology *18*, 68. https://doi.org/10.1186/s12951-020-00624-3.
30. Cheshmi, B., and Cheshomi, H. (2020). Salivary exosomes: properties, medical applications, and isolation methods. Mol. Biol. Rep. *47*, 6295–6307. https://doi.org/10.1007/s11033-020-05659-1.
31. Park, S.Y., Hwang, B.O., Lim, M., Ok, S.H., Lee, S.K., Chun, K.S., Park, K.K., Hu, Y., Chung, W.Y., and Song, N.Y. (2021). Oral-Gut Microbiome Axis in Gastrointestinal Disease and Cancer. Cancers *13*, 2124. https://doi.org/10.3390/cancers13092124.
32. Zhou, T., Xu, W., Wang, Q., Jiang, C., Li, H., Chao, Y., Sun, Y., and A, L. (2023). The effect of the "Oral-Gut" axis on periodontitis in inflammatory bowel disease: A review of microbe and immune mechanism associations. Front. Cell. Infect. Microbiol. *13*, 1132420. https://doi.org/10.3389/fcimb.2023.1132420.
33. Atarashi, K., Suda, W., Luo, C., Kawaguchi, T., Motoo, I., Narushima, S., Kiguchi, Y., Yasuma, K., Watanabe, E., Tanoue, T., et al. (2017). Ectopic colonization of oral bacteria in the intestine drives T(H)1 cell induction and inflammation. Science (New York, NY) *358*, 359–365. https://doi.org/10.1126/science.aan4526.
34. Liu, Y., Xu, T., Jiang, W., Ma, Y., Zhang, Q., Chen, N., Chu, M., and Chen, F. (2023). Single-Cell Analyses of the Oral Mucosa Reveal Immune Cell Signatures. J. Dent. Res. *102*, 514–524. https://doi.org/10.1177/00220345221145903.
35. Cao, X. (2017). Intestinal inflammation induced by oral bacteria. Science (New York, NY) *358*, 308–309. https://doi.org/10.1126/science.aap9298.
36. Elmaghrawy, K., Hussey, S., and Moran, G.P. (2020). The Oral Microbiome in Pediatric IBD: A Source of Pathobionts or Biomarkers? Front. Pediatr. *8*, 620254. https://doi.org/10.3389/fped.2020.620254.
37. Zhang, H.N., Zhou, X.D., Xu, X., and Wang, Y. (2019). [Oral microbiota and inflammatory bowel disease]. Hua xi kou qiang yi xue za zhi *37*, 443–449. https://doi.org/10.7518/hxkq.2019.04.020.
38. Li, C.J., Fang, Q.H., Liu, M.L., and Lin, J.N. (2020). Current understanding of the role of Adipose-derived Extracellular Vesicles in Metabolic Homeostasis and Diseases: Communication from the distance between cells/tissues. Theranostics *10*, 7422–7435. https://doi.org/10.7150/thno.42167.
39. Jarmalavičiūtė, A., and Pivoriūnas, A. (2016). Exosomes as a potential novel therapeutic tools against neurodegenerative diseases. Pharmacol. Res. *113*, 816–822. https://doi.org/10.1016/j.phrs.2016.02.002.
40. Shah, N., Ishii, M., Brandon, C., Ablonczy, Z., Cai, J., Liu, Y., Chou, C.J., and Rohrer, B. (2018). Extracellular vesicle-mediated long-range communication in stressed retinal pigment epithelial cell monolayers. Biochim. Biophys. Acta, Mol. Basis Dis. *1864*, 2610–2622. https://doi.org/10.1016/j.bbadis.2018.04.016.
41. Li, K., Lin, Y., Luo, Y., Xiong, X., Wang, L., Durante, K., Li, J., Zhou, F., Guo, Y., Chen, S., et al. (2022). A signature of saliva-derived exosomal small RNAs as predicting biomarker for esophageal carcinoma: a multicenter prospective study. Mol. Cancer *21*, 21. https://doi.org/10.1186/s12943-022-01499-8.
42. Ocansey, D.K.W., Zhang, L., Wang, Y., Yan, Y., Qian, H., Zhang, X., Xu, W., and Mao, F. (2020). Exosome-mediated effects and applications in inflammatory bowel disease. Biol. Rev. Camb. Philos. Soc. *95*, 1287–1307. https://doi.org/10.1111/brv.12608.
43. Liu, L., Liang, L., Yang, C., Zhou, Y., and Chen, Y. (2021). Extracellular vesicles of Fusobacterium nucleatum compromise intestinal barrier through targeting RIPK1-mediated cell death pathway. Gut Microb. *13*, 1–20. https://doi.org/10.1080/19490976.2021.1902718.
44. Cai, X., Zhang, Z.Y., Yuan, J.T., Ocansey, D.K.W., Tu, Q., Zhang, X., Qian, H., Xu, W.R., Qiu, W., and Mao, F. (2021). hucMSC-derived exosomes attenuate colitis by regulating macrophage pyroptosis via the miR-378a-5p/NLRP3 axis. Stem Cell Res. Ther. *12*, 416. https://doi.org/10.1186/s13287-021-02492-6.
45. Fizanne, L., Villard, A., Benabbou, N., Recoquillon, S., Soleti, R., Delage, E., Wertheimer, M., Vidal-Gómez, X., Oullier, T., Chaffron, S., et al. (2023). Faeces-derived extracellular vesicles participate in the onset of barrier dysfunction leading to liver diseases. J. Extracell. Vesicles *12*, e12303. https://doi.org/10.1002/jev2.12303.
46. Halfvarson, J., Brislawn, C.J., Lamendella, R., Vázquez-Baeza, Y., Walters, W.A., Bramer, L.M., D'Amato, M., Bonfiglio, F., McDonald, D., Gonzalez, A., et al. (2017). Dynamics of the human gut microbiome in inflammatory bowel disease. Nat. Microbiol. *2*, 17004. https://doi.org/10.1038/nmicrobiol.2017.4.
47. Franzosa, E.A., Sirota-Madi, A., Avila-Pacheco, J., Fornelos, N., Haiser, H.J., Reinker, S., Vatanen, T., Hall, A.B., Mallick, H., McIver, L.J., et al. (2019). Gut microbiome structure and metabolic activity in inflammatory bowel disease. Nat. Microbiol. *4*, 293–305. https://doi.org/10.1038/s41564-018-0306-4.
48. Pickard, J.M., Zeng, M.Y., Caruso, R., and Núñez, G. (2017). Gut microbiota: Role in pathogen colonization, immune responses, and inflammatory disease. Immunol. Rev. *279*, 70–89. https://doi.org/10.1111/imr.12567.
49. Clemente, J.C., Manasson, J., and Scher, J.U. (2018). The role of the gut microbiome in systemic inflammatory disease. BMJ (Clinical research ed) *360*, j5145. https://doi.org/10.1136/bmj.j5145.
50. Qu, S., Fan, L., Qi, Y., Xu, C., Hu, Y., Chen, S., Liu, W., Liu, W., and Si, J. (2021). Akkermansia muciniphila Alleviates Dextran Sulfate Sodium (DSS)-Induced Acute Colitis by NLRP3 Activation. Microbiol. Spectr. *9*, e0073021. https://doi.org/10.1128/Spectrum.00730-21.
51. Wang, L., Tang, L., Feng, Y., Zhao, S., Han, M., Zhang, C., Yuan, G., Zhu, J., Cao, S., Wu, Q., et al. (2020). A purified membrane protein from Akkermansia muciniphila or the pasteurised bacterium blunts colitis associated tumourigenesis by modulation of CD8(+) T cells in mice. Gut *69*, 1988–1997. https://doi.org/10.1136/gutjnl-2019-320105.
52. Greenhill, C. (2011). IBD: Modified Lactobacillus acidophilus may regulate intestinal inflammation. Nat. Rev. Gastroenterol. Hepatol. *8*, 182. https://doi.org/10.1038/nrgastro.2011.26.
53. von Schillde, M.A., Hörmannsperger, G., Weiher, M., Alpert, C.A., Hahne, H., Bäuerl, C., van Huynegem, K., Steidler, L., Hrncir, T., Pérez-Martínez, G., et al. (2012). Lactocepin secreted by Lactobacillus exerts anti-inflammatory effects by selectively degrading proinflammatory chemokines. Cell Host Microbe *11*, 387–396. https://doi.org/10.1016/j.chom.2012.02.006.
54. Yang, C., Zhang, M., Sung, J., Wang, L., Jung, Y., and Merlin, D. (2020). Autologous Exosome Transfer: A New Personalised Treatment Concept to Prevent Colitis in a Murine Model. J. Crohns Colitis *14*, 841–855. https://doi.org/10.1093/ecco-jcc/jjz184.
55. Leoni, G., Neumann, P.A., Kamaly, N., Quiros, M., Nishio, H., Jones, H.R., Sumagin, R., Hilgarth, R.S., Alam, A., Fredman, G., et al. (2015). Annexin A1-containing extracellular vesicles and polymeric nanoparticles promote epithelial wound repair. J. Clin. Invest. *125*, 1215–1227. https://doi.org/10.1172/jci76693.
56. Mitsuhashi, S., Feldbrügge, L., Csizmadia, E., Mitsuhashi, M., Robson, S.C., and Moss, A.C. (2016). Luminal Extracellular Vesicles (EVs) in Inflammatory Bowel Disease (IBD) Exhibit Proinflammatory Effects on Epithelial Cells and Macrophages. Inflamm. Bowel Dis. *22*, 1587–1595. https://doi.org/10.1097/mib.0000000000000840.

STAR★METHODS

KEY RESOURCES TABLE

REAGENT or RESOURCE	SOURCE	IDENTIFIER
Antibodies		
Anti-ZO1 tight junction antibody	Abcam	Cat# ab96587; RRID: AB_10680012
β-actin	Abcam	Cat# ab8227; RRID: AB_2305186
Caspase-3	Abcam	Cat# ab184787; RRID: AB_2827742
NF-κB p65	Cell Signaling Technology	Cat# 8242S; RRID: AB_10859369
Phospho-NF-κB p65	Cell Signaling Technology	Cat# 3033S; RRID: AB_331284
IκB	Cell Signaling Technology	Cat# 9242S; RRID: AB_331623
Phospho-IκBα	Cell Signaling Technology	Cat#2859S; RRID: AB_561111
FITC anti-mouse CD45	Biolegend	Cat# 157214; RRID: AB_2894427
Brilliant Violet 421 anti-mouse F4/80	Biolegend	Cat# 123131; RRID: AB_10901171
PerCP/Cyanine5.5 anti-mouse/human CD11b	Biolegend	Cat# 101228; RRID: AB_893232
APC anti-mouse CD86	Biolegend	Cat# 105012; RRID: AB_493342
PE anti-mouse CD206	Biolegend	Cat# 141706; RRID: AB_10895754
Anti-CD68 antibody	Abcam	Cat# ab125212; RRID: AB_10975465
Anti-CD63 antibody	Abcam	Cat# ab134045; RRID: AB_2800495
Anti-TSG101 antibody	Abcam	Cat# ab125011; RRID: AB_10974262
Anti-CD9 antibody	Abcam	Cat# ab223052; RRID: AB_2922392
Biological samples		
Mice fecal samples	This study	N/A
Mice colon tissue	This study	N/A
Human saliva	This study	N/A
Chemicals, peptides, and recombinant proteins		
RPMI 1640	Gbico	Cat# C11875500BT
Fetal Bovine Serum (FBS)	Invitrogen	Cat# 10099141C
HEPES	Gbico	Cat# 15630130
EDTA	Invitrogen	Cat# AM9260G
Trypsin	Thermo Fisher	Cat# 25200056
Deoxyribonuclease I	Sigma	Cat# DN25-1G
Collagenase Type VIII	Sigma	Cat# C2139-5G

(*Continued on next page*)

Continued

REAGENT or RESOURCE	SOURCE	IDENTIFIER
Percoll	Sigma	Cat# GE17-0891-09
Dextran Sulfate Sodium Salt	MP Biomedicals	Cat# 0216011090
Phosphate Buffered Saline (PBS)	Solarbio	Cat# P1020
Penicillin-Streptomycin Mixed	Invitrogen	Cat# 15140122
DNase/RNase-Free Water	Solarbio	Cat# R1600
DMEM	Invitrogen	Cat# C11995500BT
Lipopolysaccharides from Escherichia coli (LPS)	Sigma	Cat# L2630
Trizol reagent	Thermo Fisher	Cat# 15596018
PowerUp™ SYBR™ Green	Thermo Fisher	Cat# A25742
Phusion High-Fidelity PCR Master Mix	New England Biolabs	Cat# M0532S
Protease and Phosphatase Inhibitor Cocktail	Thermo Fisher	Cat# 78440
Critical commercial assays		
Human IL-6 ELISA Kit	MultiSciences	Cat# 70-EK106/2-24
Human IL-1β ELISA Kit	MultiSciences	Cat# 70-EK101B-24
Human TNF-a ELISA Kit	MultiSciences	Cat# 70-EK182-24
NEBNext Ultra II DNA Library Prep Kit	NEB	Cat# E7645L
QIAquick Gel Extraction Kit	QIAGEN	Cat# 28706
Universal two-step detection kit	ZSGB-BIO	Cat# PV-9000
Deposited data		
16S rRNA gene sequencing data	This study	GSA: CRA017599
MicroRNA sequencing data	This study	GSA-Human: HRA007892
Experimental models: Cell lines		
Caco-2	ATCC	Cat# HTB-37
THP-1	ATCC	Cat# TIB-202
Experimental models: Organisms/strains		
C57BL/6 mice	SPF(Beijing) Vital River Laboratory Animal Technology Co., Ltd.	N/A
Oligonucleotides		
Primers for quantitative PCR, see Table S2	This paper	N/A
Software and algorithms		
GraphPad Prism 7.0	GraphPad Software	N/A
ImageJ software	National Institutes of Health	N/A
FASTP software	FASTP software	N/A
Vsearch software	Vsearch software	N/A
FlowJo v10.8.1 software	FlowJo LLC	N/A

EXPERIMENTAL MODEL AND STUDY PARTICIPANT DETAILS

Ethics approval and consent to participate

The salivary exosomes of IBD patients with different subtypes and disease states may differ. For our cohort, we included saliva extracts from CD individuals (n = 47) and UC (n = 58). Control group contained 25 donors without any history for IBD or other immune-mediated inflammatory diseases. Patient samples were performed with approval from the Ethics Committee at the Peking university people's hospital (2021PHB107 AND 2022PHB373), and all participants provided written informed consent. As presented in Tables 1 and S1, 105 patients with active IBD (n = 62, 39 UC and 23 CD, 28 females, and 30 males) or in remission (n = 43, 19 UC and 24 CD, 13 females, and 30 males) were included. Disease activity scores and recognized inflammatory biomarkers (CRP and ESR) were recorded, as well as standard treatments and whether surgical treatment was performed. Since some of the patients did not undergo serological testing when their saliva was collected, the number of people who underwent testing is indicated in the table. Prior to sampling, subjects were instructed to clean their

oral cavity and to abstain from food and water for at least one hour to minimize dietary and fluid intake effects on the sample's composition. After a 15-minute rest period in a quiet room, participants were asked to sit in a relaxed position, with their tongue pressed against the palate and their head naturally inclined to allow the natural flow of saliva. Saliva was collected passively in a 50 mL centrifuge tube, with a target volume of approximately 5 mL. Immediately following collection, entire saliva extracts receiving no stimulation were retained on ice, and then centrifugated (3000 ×g, 20 minutes, 4°C) to eliminate insoluble debris, material, and cells from the samples. For subsequent experiments, the saliva supernatant was temporarily kept in a refrigerator at -80°C.

Animal model and treatment

Male C57BL/6 mice (6 to 8 weeks of age) were reared in the SPF animal laboratory of Peking University People's Hospital. All animal experiments were reviewed and approved by the Institutional Animal Care and Use Committee at Peking university people's hospital prior to the initiation of any studies (2021phe036). Mice were randomly segregated into 7 groups ($n = 3 \sim 4$/group): active UC patients' salivary exosomes + DSS(UC/A salivary Exo+ DSS), salivary exosomes isolated from UC patients in remission + DSS(UC/R salivary Exo+ DSS), active CD patients' salivary exosomes+ DSS (CD/A salivary Exo + DSS), salivary exosomes isolated from CD patients in remission + DSS (CD/R salivary Exo + DSS), healthy control' salivary exosomes + DSS(HC salivary Exo + DSS), as well as mice were given PBS by gavage + DSS (PBS + DSS) and the normal group without DSS(N). For five days, mice were given 1.5% DSS (MP Biomedicals dissolved in water). After a subsequent five-day administration of standard water, they were executed for future experiments (Figure S9). The amount of saliva secretion can be estimated by the amount of drinking water. For example, the daily amount of human saliva is about 1-1.5L, the amount of drinking water is about 1-2L, and the daily amount of drinking water of mice is about 5-10 mL. According to our experiment, each milliliter of saliva contains about 7-10ug of exosomes, so we gave 50 μg of salivary exosomes to each mouse every day.

Cell culturing

Human myeloid leukemia mononuclear cells (THP-1 cells) and human colorectal adenocarcinoma cells (Caco2 cells) were provided by the Department of Gastroenterology, Peking University People's Hospital. THP-1 cells grown in RPMI 1640 medium (Gbico) supplemented with 10% fetal bovine serum (FBS; Invitrogen) at 37°C in 5% CO_2. Caco2 cells were cultured in DMEM medium (Invitrogen) supplemented with 10% FBS at 37°C in 5% CO_2. THP-1 cells were stimulated with 100 ng/mL PMA (Sigma) for 24 hours to induce a macrophage-like phenotype before conducting cell experiments. Caco2 cells were treated with 1 μg/mL LPS and 40 μg/mL of salivary exosomes simultaneously. After 24 hours of co-culture, cells and supernatants were isolated for subsequent examination.

METHOD DETAILS

IBD diagnosis and activity

Diagnosis for IBD and subtype was confirmed by clinical manifestation, endoscopy, and histology. Disease activity was determined by clinical manifestation and endoscopic appearance. CD activity was evaluated with CDAI, including height, weight, hematocrit, symptoms, and complications, etc. Ant CDEI was introduced to assist in the assessment of endoscopy activity. Therefore, the active CD was determined by CDAI $\geq$150 or CDEI $\geq$5. For patients divided into UC subtypes, modified Mayo disease activity index containing bowel frequency, rectal hemorrhaging, assessment by a doctor, and endoscopy findings. Mayo score $\geq$3 was determined as active UC.

Extraction and classification of salivary exosomes

Saliva was centrifuged (12,000 × g, 20 minutes, 4°C) to remove vacuoles. After being passed through filters (0.22 μm, Millipore), the supernatant was centrifuged again (120,000 × g ,70 minutes, 4°C) to pellet the exosomes (Beckman Coulter, SW32 Ti). A large volume of PBS was then used to wash the resulting pellet, and then ultracentrifuged again under the same conditions, to prepare exosomes. The nanoparticle tracing analysis approach (Flow NanoAnalyzer) was employed to characterize the purified exosomes, and the structure of the exosomes was assessed utilizing transmission electron microscopy (TEM) (JEM-2000EX TEM). Western blotting was conducted to identify three established exosome indicators (Tsg101, CD9, CD63). Counting of the exosomes was performed utilizing a Micro BCA™ Protein Assay Kit (Thermo Fisher). he extracted exosomes were kept at -80°C for subsequent experimentation.

RNA extraction and real-time quantitative PCR (qRT-PCR)

RNA was extracted from the mouse colon and cells utilizing Trizol (Thermo Fisher) and chloroform extraction. The concentrations and purities of the extracted RNAs were identified using a NanoDrop (ND-2000, Thermo Fisher). A RevertAid First Strand cDNA Synthesis Kit (Applied Biosystems) was utilized to produce the cDNA following to the manufacturer's directions. The target gene levels were characterized via real-time quantitative PCR using SYBR®Green (Thermo Fisher). Relative mRNA levels were standardized to GAPDH and characterized by the $2^{-\Delta\Delta Ct}$ method. All primers utilized are outlined in Table S2.

Western blotting

The protein samples were lysed using enhanced RIPA Lysis Buffer (APPLYGEN, Beijing) and a protease & phosphatase inhibitor cocktail (100X) (Thermo Fisher). Subsequently, the membranes were blocked with 5% w/v skimmed milk (BD Biosciences) in Tris-buffered saline supplemented with 0.1% v/v Tween 20 (TBST) for one hour at room temperature. Overnight incubation at 4 °C was then performed with the following

primary antibodies: anti-CD9 (1:200, Abcam), anti-CD63 (1:200, Abcam), anti-TSG101 (1:1000, Abcam), anti-IκB-α (1:500, CST), anti-p-IκB-α (1:500, CST), anti-NF-κB p65 (1:500, CST), anti-NF-κB p-p65 (1:500, CST), anti-zo-1 (1:1000, Abcam), anti-caspase-3 (1:500, CST), and β-actin (1:1000, Abcam).The secondary antibodies (1:2500, ZSGB-BIO) were added and incubated for one hour. Precise bands were characterized using ECL Blotting Detection Reagents (Thermo Fisher).

Animal live imaging analysis

Salivary exosomes were tagged using a lipophilic dye, DIL (Thermo Thermo Fisher), adhering to the manufacturer's recommendations for viewing. DIL-labeled salivary exosomes were given to C57BL/6 mice by gavage. After 6 hours, the scattering of fluorescence in mice was examined using an *in vivo* imaging approach (IVIS Spectrum).

Flow cytometric analysis

Isolation of immune cells from colonic lamina propria (LPCs), to quantify immune cells, single-cell suspensions isolated from LPCs were given anti-mouse CD16/ 32 FcR blockade and stained using fluorescence-tagged antibodies (Biolegend, USA). Fluorescence was characterized and recorded using flow cytometry (BD Celesta), and raw data were further assessed and pictured by FlowJo v10.8.1.

Enzyme-linked immunosorbent assay (ELISA)

Supernatants were harvested to detect TNF-α, IL-6, and IL-1β. ALL ELISA kits were from Multisciences. The specific experimental process was carried out according to the kit's protocol. Dual-wavelength detection was performed using a Multiskan GO Microplate Reader (Thermo Fisher). To find the OD_{450} and OD_{570} or OD_{630}, the calibrated OD was calculated as the 450 nm measured value minus the 570 nm or 630 nm measured value. All methods were performed according to the manufacturer's instructions.

Hematoxylin and eosin (H&E) staining and histopathological evaluation

A segment of mouse colorectal tissue was fixed using 4% paraformaldehyde (pH 7.4), dehydrated with a series of ethanol, embedded in paraffin, sectioned into 5-μm slices, stained with H&E, and finally mounted and scanned using an Upright fluorescence microscope (ZEISS). Histopathology scores were validated in colonic segments by two blinded trained pathologists, with an integrated score for inflammatory cell infiltration (Score, 0-3) and tissue damage (Score, 0-3).

Immunohistochemistry (IHC)

The tissue implanted in paraffin underwent fixing and dewaxing, and the sections were placed in a preheated antigen repair solution (sodium citrate pH 6.0) and restored for 11 mins on high heat in the microwave oven, twice in total. Then, it was followed by endogenous peroxidase blocking for 10 minutes (room temperature). Tissues were incubated alongside a 5% BSA solution for one hour to preclude non-specific antigen binding. The tissues were housed with anti-CD68 (1:500; Abcam) (4°C, overnight), the enhanced reaction fluid, and the secondary antibody (ZSGB-BIO) following the producer's recommendations. Thereafter, tissue staining with DAB (ZSGB-BIO) was utilized, and resin was used to seal. The count of positive cells within the mucosal section was determined by microscope (ZEISS) observation and image collection.

Microbiota 16S rRNA gene sequencing

Total DNA isolated from mouse feces followed the SDS method. 16S rRNA genes across specific regions (16S V3-V4) were amplified using specific primers and barcodes. All PCR reactions comprised 15 μL of Phusion® High-Fidelity PCR Master Mix (New England Biolabs). PCR products were combined in equal quantities, and purified via a Qiagen Gel Extraction Kit (Qiagen, Germany). Sequencing libraries were developed using the NEBNext® Ultra™ IIDNA Library Prep Kit, and their quality was examined using a Qubit@ 2.0 Fluorometer (Thermo Fisher) and Agilent Bioanalyzer 2100 system. Sequencing was performed on an Illumina NovaSeq platform, producing 250 bp paired-end reads. Based on the barcode and primer sequence, each sample was differentiated. Following the trimming of barcode and primers, obtaining Raw Tags. FASTP software was used to acquire Raw Tags quality control and acquire high-quality Clean Tags. Ultimately, Vsearch software was employed to contrast Clean Tags with the database to validate and excise chimeras, generating valid data for subsequent analysis.

QUANTIFICATION AND STATISTICAL ANALYSIS

The data are presented as mean ± standard error of the mean (SEM). Multiple group comparisons of data that adhered to a normal distribution were performed using one-way ANOVA. Post-hoc pairwise comparisons were conducted using the Least Significant Difference (LSD) method. Data that did not conform to a normal distribution were analyzed using non-parametric tests. Significance levels (P values) are indicated in legends of each figure, showing *, $p < 0.05$; **, $p < 0.01$; ***, $p < 0.001$; ****, $p < 0.0001$; ns, non-significant. All results of *in vitro* experiments were collected from at least 3 independent biological replicates.